An enhanced coupled ISPH-TLSPH FSI solver by a Riemann fluid-structure acceleration scheme

Takafumi Gotoh*, Abbas Khayyer, Hitoshi Gotoh
Department of Civil and Earth Resources Engineering
Kyoto University
Kyoto, Japan
taka.gotoh@ku.pmres.jp

I. Introduction

In the field of engineering, severe interactions between fluids and structures are often encountered. Specific examples include interactions between violent fluids and floating objects such as small ships, associated with global warming, interactions between water flow and gates or turbines in hydraulic power generators, and blood flow through blood vessels that expand and contract accordingly. In order to reveal these phenomena and contribute to design and operation, the development and application of highly accurate fluid-structure interaction (FSI) solver is anticipated.

In particular, the interface between the fluid and the structure is a discontinuous surface of the material, and it is necessary to connect the fluid and the structure in a consistent manner. Various methods with the SPH method have been developed so far. Regarding methods employing a projection-based fluid model, Khayyer et al. [1] proposed the Fluid-Structure Acceleration-based (FSA) coupling scheme. This method is effective without any additional stabilisation process. Hwang et al. [2] implemented the Pressure Integration (PI) coupling scheme (originally proposed by Antoci et al. [3]), which calculates the interaction force based on the approximate SPH evaluation of the surface integral of the fluid pressure at the interface. While this method is widely applicable, it is vulnerable to instability due to pressure fluctuations. Morikawa and Asai [4] incorporated the viscous term and applied the momentum-conserving pressure gradient interaction force, but they also introduced a stabilisation term additionally for the stable calculation. However, with the previous methods, unless an additional artificial stabilisation term is added, there is a possibility that noise would occur in the simulated physical quantities, such as the pressure field, at and in the vicinity of the interface, and that this would have a negative impact on the behaviour of the entire system.

Therefore, in this study, targeting the ISPH-TLSPH coupling solver, a novel FSI coupling scheme including a Riemann-based stabilisation term is proposed to ensure stability and more importantly a physically consistent transfer of momentum from fluid to structure and vice versa. In addition, the VEM (Velocity divergence Error Mitigating) scheme [5, 6] is reformulated and incorporated to further stabilise the fluid-structure interface.

II. Numerical Method

A. Fluid model

The fluid is considered to be incompressible and inviscid, therefore, the fluid phase governing equations are expressed as:

$$\nabla\cdot\boldsymbol{u}=0,\quad \frac{D\boldsymbol{u}}{Dt}=-\frac{1}{\rho}\nabla p+\boldsymbol{g}+\boldsymbol{a}^{\mathrm{SF}},\tag{1}$$

where, $\boldsymbol{u}$: velocity, t: time, ρ : density, p : pressure, $\boldsymbol{g}$: gravitational acceleration, and $\boldsymbol{a}^{\mathrm{SF}}$: interaction acceleration from the structure.

In the ISPH method, projection method is adopted to solve these governing equations. In each time step k, after updating the velocity and position by gravitational acceleration, the following Poisson Pressure Equation (PPE) taking into account the incompressibility conditions is solved in an implicit manner.

$$\langle\nabla^2 p_{k+1}\rangle_i=\frac{1}{\Delta t}\left(\frac{D\rho}{Dt}\right)_i^*,\tag{2}$$

where, Δt: time step size, superscript $*$: the value just before the PPE solution step, subscript i: target particle.

B. Structure model

The governing equation of the TLSPH structure model is the following equation of motion.

$$\frac{D\boldsymbol{u}}{Dt}=\frac{1}{\rho_0}\nabla_0\cdot\boldsymbol{P}+\boldsymbol{g}+\boldsymbol{a}^{\mathrm{FS}},\tag{3}$$

where, $\boldsymbol{P}$: the first Piola-Kirchhoff stress tensor, $\boldsymbol{a}^{\mathrm{FS}}$: interaction acceleration from the fluid, and subscript 0: the value with respect to initial configuration. Here, the neo-Hookean constitutive model is adopted targeting hyperelastic materials:

$$\boldsymbol{P}=\mu(\boldsymbol{F}-\boldsymbol{F}^{-\mathrm{T}})+\lambda\ln(J)\boldsymbol{F}^{-\mathrm{T}},\ \boldsymbol{F}=\nabla_0\boldsymbol{r},\ J=\det\boldsymbol{F},\tag{4}$$

where, $\boldsymbol{F}$: the deformation gradient tensor, μ and λ: the Lame's constants, J: Jacobian, $\boldsymbol{r}$: the current position vector, and the superscript $-\mathrm{T}$: the inverse of a transposed tensor.

In TLSPH discretisation employed here, second-order accuracy (referred to as "C2nd") is ensured for accurate simulations, and the "complete Riemann (cR)" diffusion term is employed to suppress the rank deficiency with a minimal dissipation [7].

C. Fluid-structure coupling

In the conventional FSA coupling scheme [1], the PPE of the fluid is first solved by treating the structural particles as moving wall boundaries, and then the acceleration term of the structural particles due to the adjacent fluid particles is obtained from the gradient of the pressure solution of the PPE calculated at the position of the structural particles. Specific formulation in FSA is as follows.

$$\boldsymbol{a}_i^{\mathrm{FS}} = -\frac{1}{\rho^{\mathrm{S}}}\sum_j V_j\left(p_j - p_i\right)\boldsymbol{C}_i \cdot \nabla w_{ij}, \quad (5)$$

where, superscript S : the value of structure, subscript j : neighbouring particle, V: the volume of particle, w: kernel (C2 Wendland kernel adopted in this study), and $\boldsymbol{C}_i$: the correction matrix to ensure the first-order Taylor series consistency.

Although the FSA is designed to ensure continuity of normal stress (only accounting for the spherical part of the stress tensor) and velocity at the interface, a physically consistent transfer of momentum from fluid to structure and vice versa is not necessarily guaranteed, particularly, in presence of instabilities in reproduced physical fields, such as pressure and velocity fields.

Therefore, in this study, a Riemann-based interaction term is proposed to ensure stability and a physically consistent momentum transfer between fluid and structure. Specific formulation is as follows, referring to [8-10].

$$\boldsymbol{a}_i^{\mathrm{FS}} = -\frac{1}{\rho^{\mathrm{S}}}\sum_j 2p^* V_j \nabla w_{ij}, \; p^* = \bar{p} + \frac{1}{2}\beta\bar{\rho}c_0\left(u_i - u_j\right),$$

$$\bar{p} = \frac{p_i + p_j}{2}, \; \bar{\rho} = \frac{\rho_i + \rho_j}{2}, \; u_i = \boldsymbol{u}_i \cdot \frac{\boldsymbol{r}_{ij}}{r_{ij}}, \; u_j = \boldsymbol{u}_j \cdot \frac{\boldsymbol{r}_{ij}}{r_{ij}}, \quad (6)$$

where, β : a limiter function, and c_0 : sound speed. This formulation enhances the momentum conservation at the interface while mitigating the problem caused by kinematic discontinuities.

Furthermore, in order to suppress instabilities associated with kinematic discontinuities and further stabilise the interface, the following VEM scheme [5, 6] is additionally activated for the interaction acceleration.

$$\boldsymbol{a}_i^{\mathrm{VEM}} = -\frac{1}{\rho_i}\sum_j V_j F\left(p_j^{\mathrm{VEM}}, p_i^{\mathrm{VEM}}\right)\nabla w_{ij},$$

$$F\left(p_j^{\mathrm{VEM}}, p_i^{\mathrm{VEM}}\right) = \begin{cases} p_j^{\mathrm{VEM}} + p_i^{\mathrm{VEM}} & \left(p_i^{\mathrm{VEM}} \geq 0\right) \\ p_j^{\mathrm{VEM}} - p_i^{\mathrm{VEM}} & \left(p_i^{\mathrm{VEM}} < 0\right) \end{cases},$$

$$p_i^{\mathrm{VEM}} = -\rho_i C h |\boldsymbol{u}|_{\max} \langle \nabla \cdot \boldsymbol{u} \rangle_i, \quad (7)$$

where, C: coefficient (set to 5), h: smoothing length of kernel, and $|\boldsymbol{u}|_{\max}$: maximum velocity. Here the VEM scheme acts as a designed diffusive term as a function of velocity divergence field to stabilise the interface.

III. Numerical Investigation and Validation

The proposed ISPH-TLSPH FSI solver is qualitatively and quantitatively validated through the simulation of dambreak with an elastic plate [11, 12]. The initial water column height is $H = 0.40$ m and the width is $L = 0.20$ m. The density of the water is $\rho^F = 997$ kg/m^3. The Young's modulus of the elastic plate is $E^S = 3.5\mathrm{E}{+}6$ Pa, and the density is $\rho^S = 1161.54$ kg/m^3. A displacement measurement point P is set on the plate at a height of 0.0875m.

Fig. 1 (a) presents the pressure field of the fluid and the shear stress distribution of the elastic plate at time $t = 0.80$s (the fluid-structure interface is indicated with black lines) for the cases with the FSA, additional VEM activation at the interface, and the Riemann-based interaction term and VEM. **Fig. 1 (b)** shows the experimental result at the same instant [12]. Focusing on the deformation of the elastic plate, the shape in the FSA case is different from the experimental results, but by adding VEM and employing a Riemann-based interaction term together with VEM, results close to the experiment are obtained. Also, comparing the enlarged view around the bottom of the elastic plate displayed in the lower left of the figure, in case of FSA **(i)**, a void space is formed between the plate and the fluid, and noise can be seen in the distribution of physical quantities. By adding VEM at the interface **(ii)**, the void space is eliminated, but the pressure distribution is still a little disturbed. On the other hand, by employing the Riemann-based interaction term together with VEM **(iii)**, a smooth pressure field is obtained. In other words, the results are enhanced, as the instability associated with the kinematic discontinuity is mitigated by VEM and a physically consistent transfer of momentum at the interface is enhanced by the Riemann-based interaction term.

Fig. 1 (c) compares the time histories of the displacement of the elastic plate for the three cases shown in the snapshot and the experimental result. By incorporating the Riemann-based interaction term and VEM, calculation results closer to the experiment are obtained in the latter part of the simulation (after $t = 0.80$s).

IV. Concluding Remarks

In this study, an enhanced ISPH-TLSPH hyperelastic FSI solver is proposed. The TLSPH structure model incorporates recently developed C2nd (second-order Consistency) and cR (complete Riemann) schemes for accurate simulation of non-linear and finite strain elastic structural responses. To ensure fluid-structure interface stability and physical transfer of momentum between different phases a novel FSI coupling

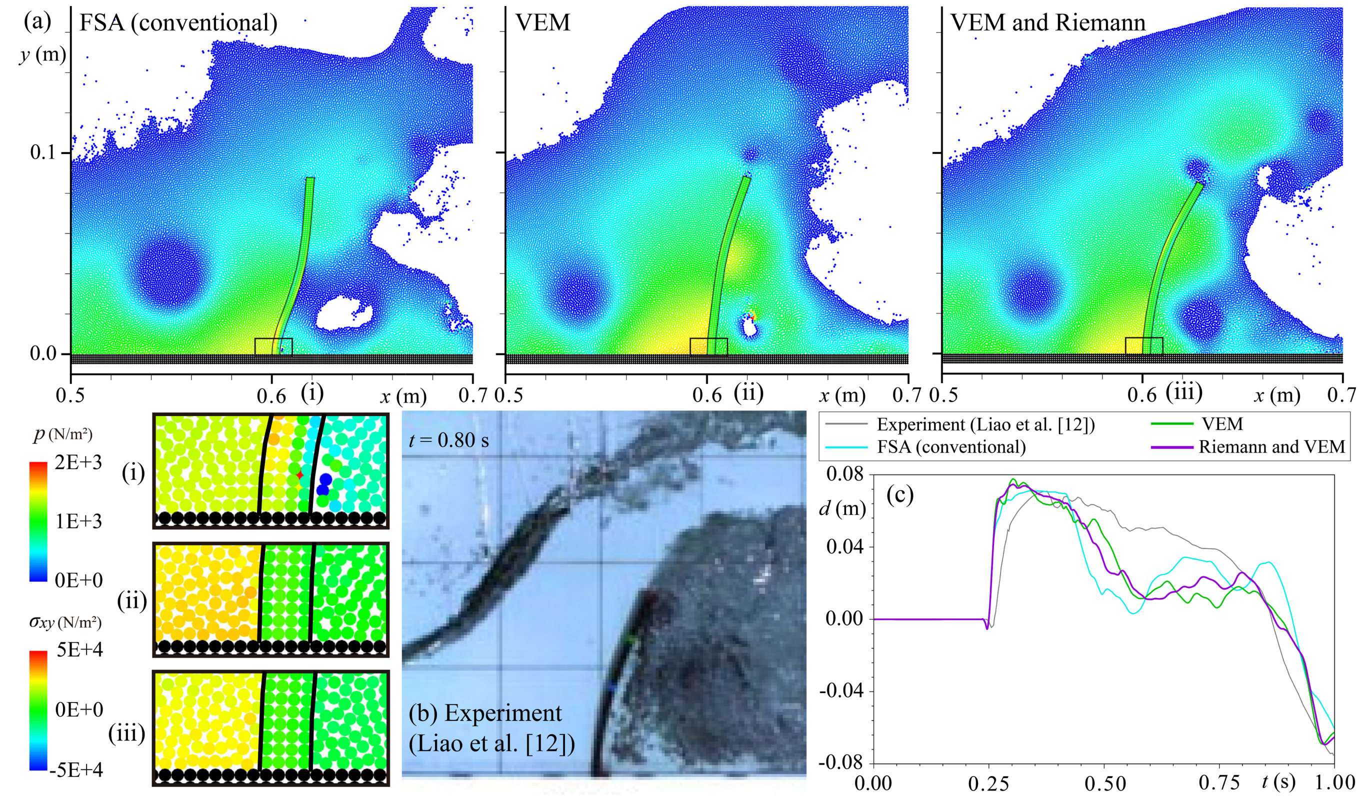

Figure 1. The simulation results of dambreak with an elastic plate **(a)** Pressure field of the fluid and the shear stress distribution of the elastic plate at time t = 0.80 s (the fluid-structure interface is indicated with black lines) for the cases with the FSA, additional VEM activation at the interface, and the Riemann-based interaction term and VEM, **(b)** The experimental result at the same instant [12], **(c)** Comparison of the time histories of the displacement of the elastic plate at the displacement measurement point P

scheme including a Riemann term is proposed. In addition, a modified VEM scheme for the interface is presented for further stabilisation associated with interfacial kinematic discontinuity. Through the simulation of dambreak with an elastic plate, it is shown that the incorporation of the Riemann-based fluid-structure interaction term together with the interfacial VEM stabilises the field around the fluid-structure interface and results in a more physically consistent solution. More extensive validations will be conducted and presented during the 19th SPHERIC World Conference.

Acknowledgment

This work was supported by the JST (Japan Science and Technology Agency) SPRING, Grant Number JPMJSP2110.

References

[1] A. Khayyer, H. Gotoh, H. Falahaty, and Y. Shimizu, "An enhanced ISPH–SPH coupled method for simulation of incompressible fluid–elastic structure interactions," Computer Physics Communications, vol. 232, pp. 139–164, 2018.

[2] S.C. Hwang, A. Khayyer, H. Gotoh, and J.C. Park, "Development of a fully Lagrangian MPS-based coupled method for simulation of fluid–structure interaction problems," Journal of Fluids and Structures, vol. 50, pp. 497–511, 2014.

[3] C. Antoci, M. Gallati, and S. Sibilla, "Numerical simulation of fluid–structure interaction by SPH," Computers and Structures, vol. 85, pp. 879–890, 2007.

[4] D.S. Morikawa, and M. Asai, "Coupling total Lagrangian SPH–EISPH for fluid–structure interaction with large deformed hyperelastic solid bodies," Computer Methods in Applied Mechanics and Engineering, vol. 381, No. 113832, 2021.

[5] A. Khayyer, Y. Shimizu, T. Gotoh, and H. Gotoh, "Enhanced resolution of the continuity equation in explicit weakly compressible SPH simulations of incompressible free-surface fluid flows," Applied Mathematical Modelling, vol. 116, pp. 84–121, 2023.

[6] T. Gotoh, A. Khayyer, and H. Gotoh, "Enhanced schemes for resolution of the continuity equation in projection-based SPH," Engineering Analysis with Boundary Elements, vol. 166, No. 105848, 2024.

[7] T. Gotoh, D. Sakoda, A. Khayyer, C.H. Lee, A. Gil, H. Gotoh, and J. Bonet, "An enhanced Total Lagrangian SPH for non-linear and finite strain elastic structural dynamics," Computational Mechanics (in press)

[8] A. Khayyer, H. Gotoh, Y. Shimizu, and T. Gotoh, "An improved Riemann SPH-Hamiltonian SPH coupled solver for hydroelastic fluid-structure interactions," Engineering Analysis with Boundary Elements, vol. 158, pp. 332–355, 2024.

[9] B. Bouscasse, A. Colagrossi, S. Marrone, and M. Antuono, "Nonlinear water wave interaction with floating bodies in SPH," Journal of Fluids and Structures, vol. 42, pp. 112–129, 2013.

[10] P.N. Sun, D. Le Touzé, and A.-M. Zhang, "Study of a complex fluid-structure dam-breaking benchmark problem using a multi-phase SPH method with APR," Engineering Analysis with Boundary Elements, vol. 104, pp. 240–258, 2019.

[11] K. Liao, C. Hu, and M. Sueyoshi, "Numerical Simulation of Free Surface Flow Impacting on an Elastic Plate," Abstract for the 29th Intl Workshop on Water Waves and Floating Bodies, Osaka (Japan), March 30 – April 02, 2014.

[12] K. Liao, C. Hu, and M. Sueyoshi, "Free surface flow impacting on an elastic structure: Experiment versus numerical simulation," Applied Ocean Research, vol. 50, pp. 192–208, 2015.